PROCEEDINGS, Fifteenth Workshop on Geothermal Reservoir Engineering
Stanford University, Stanford, California, January 23-25, 1990
SGP-TR-130

A Casting and Imaging Technique for Determining Void Geometry and Relative Permeability Behavior of a Single Fracture Specimen

B. L. Cox, K. Pruess, and P. Persoff

Earth Sciences Division
Lawrence Berkeley Laboratory
University of California
Berkeley, California 94720

ABSTRACT

A casting technique has been developed for making translucent replicas of the void space of natural rock fractures. Attenuation of light shined through the cast combined with digital image analysis provides a pointwise definition of fracture apertures. The technique has been applied to a fracture specimen from Dixie Valley, Nevada, and the measured void space geometry has been used to develop theoretical predictions of two-phase relative permeability. A strong anisotropy in relative permeabilities has been found, which is caused by highly anisotropic spatial correlations among fracture apertures.

INTRODUCTION

Fluid flow in most high-temperature geothermal reservoirs is dominated by the highly permeable pathways provided by rock fractures and joints. Engineering design of geothermal production and injection operations requires an understanding of fracture flow under a wide range of conditions. Of special importance are the effective permeabilities of fractures under multiphase flow conditions, i.e., under conditions where water and steam flow simultaneously. Multiphase flow in fractures also plays an important role in oil and gas recovery from fractured reservoirs, and in planned geologic repositories for high-level nuclear wastes.

The key to understanding flow in fractures is in the geometric characteristics of the void space enclosed between the fracture walls. Traditionally, fracture flow has often been viewed in analogy to flow between parallel plates, as in a Hele-Shaw cell. Recent laboratory and field work, however, has indicated the importance of wall roughness and contacts (Brown and Scholz, 1985; Gentier, 1986; Pyrak-Nolte *et al.*, 1987; Gale, 1987; Hakami, 1988). These empirical studies of fracture void geometry have led to a conceptualization of fractures as two-dimensional heterogeneous porous media.

In the present work we apply a casting technique pioneered by Gentier *et al.*, (1989) to create a replica of the void space enclosed between the walls of actual fracture specimen. The cast of the void space consists of translucent epoxy resin, the thickness of which can be measured by means of light attenuation. Digital image analysis yields a virtually pointwise definition of fracture aperture. The casting technique for measuring fracture void space geometry has been evaluated by comparison with the older profilometer approach, with encouraging results.

The definition of void geometry obtained for a fracture specimen from Dixie Valley, Nevada, has been used in a theoretical analysis of effective fracture permeability to two fluid phases flowing simultaneously. The results for fracture relative permeabilities are compared with earlier findings for artificial computer-generated aperture distributions.

DESCRIPTION OF ROCK SPECIMEN

The fractured rock specimen was excavated from a highly altered contact between alluvial sediments and metamorphosed gabbro at a major range-front normal fault in Dixie Valley, Churchill County, Nevada. The location was in the Stillwater seismic gap near 39.95°N. Lat., 117.95°W. Long. (Power and Tullis, 1989). The rock fracture was taken from near the surface, and the fracture was closed, with a thin (1–5 mm) coating of calcite. The highly altered slickenside rock surfaces, analyzed by transmission electron microscopy, consist of approximately 98 percent fine-grained (0.01–1 mm) quartz and 2 percent kaolinite and Fe-oxide (Power and Tullis, 1989). The hydrothermal quartz represents alteration of alluvial sediments and metamorphosed Jurassic gabbroic rocks, part of a slickenside zone extending approximately 100 m along the fault zone. The quartz and kaolinite assemblage indicates that the slickenside surface must have formed at temperatures below 270°C, because above that temperature pyrophyllite would have formed (Power and Tullis, 1989). Slip along the fault may have been as great as 3–6 km, and fault surfaces now found at the surface probably formed at depths of 1–2 km (Power and Tullis, 1989). The actual in situ conditions of the fracture have changed over time, in response to changing stress and the circulation of hydrothermal fluids. The presence of slickensides indicates that at some point in the past there had been considerable wall-to-wall contact.

The surface area of the fracture specimen is an irregular shape roughly 110×110 mm^2 with orthogonal side surfaces machined perpendicular to the fracture. Power removed the calcite coating from the fracture walls, and then measured their topography using a profilometer method, utilizing a mechanical stylus which was moved along the surface in parallel profiles, digitally recording the vertical displacement. He measured apertures over an area of 83×73 mm. We obtained this specimen from him in order to have a basis of comparison for apertures obtained from the same sample using the casting method. The detailed comparison of these two methods is the subject of another paper in preparation (Cox *et al.*, 1990).

CASTING METHOD

The casting method used to make a replica of the fracture void space is described by Gentier *et al.*, (1989). The two sides of the fracture are fitted together to act as a mold in which the fracture void space is filled with a colored, translucent RTV (room temperature vulcanizing) silicone rubber (Rhone-Poulenc #1556). For calibration purposes, a wedge of known thickness is cast at the same time using the same batch of silicone material in a machined mold with a flat cover plate. The fracture and wedge mold are both filled with the RTV, and excess polymer is squeezed out by applying pressure on opposite sides of the fracture. Pressure is maintained at approximately 5000N/m^2 (0.05 bar) normal to the fracture while the silicon is cured at 100°C for 4 h. The two sides of the fracture are then carefully separated to avoid tearing the tissue-paper-thin cast, which adheres to one side of the fracture. A clear silicon rubber is poured over the cast, which when cured acts as a support for the cast, facilitating the removal of the cast from the rock, and supporting the cast during the imaging process.

Both the fracture cast (and its clear support) and the calibration wedge are placed on a light table and photographed by transmitted light using an Eiconix 78/99 AD2 digitizing camera. The camera uses a linear photodiode array to capture an image of 2048×2048 pixels, each having a light intensity between 0 and 255. Calibration of cast thickness is obtained by plotting (logarithm of) light intensity against known thickness of the calibration wedge. A 1024×1024 pixel subset corresponding approximately to the region covered by the mechanical profilometer was extracted, with each pixel representing an area of around 0.07×0.07 mm^2, better than seven times the spatial resolution of the mechanical profilometer. Surface plots of the apertures obtained from two casts were compared with the surface plots of the profilometer data set, and were very similar (Cox *et al.*, 1990).

The 1024×1024 pixel subset represents an area of 72.02×72.02 mm^2, with grid spacing of 0.07 mm, a mean aperture of 0.225 mm, and a standard deviation of 0.05 mm. The aperture correlation length was estimated to range between 5 and 15 mm from statistical correlograms as well as a visual inspection of the topography. Therefore, a much coarser discretization was expected to be sufficient to adequately represent the fracture void space geometry. By averaging over 32×32 pixel subsets the data were reduced to a 32×32 (2.3 mm spacing) set. Figure 1 shows that the cumulative aperture frequency distribution from this reduced set agrees well with the distribution from the original 1024×1024 set. A contour plot of fracture apertures is shown on Fig. 2. The 32×32 discretized aperture distribution plotted into five size categories is shown on Fig. 3.

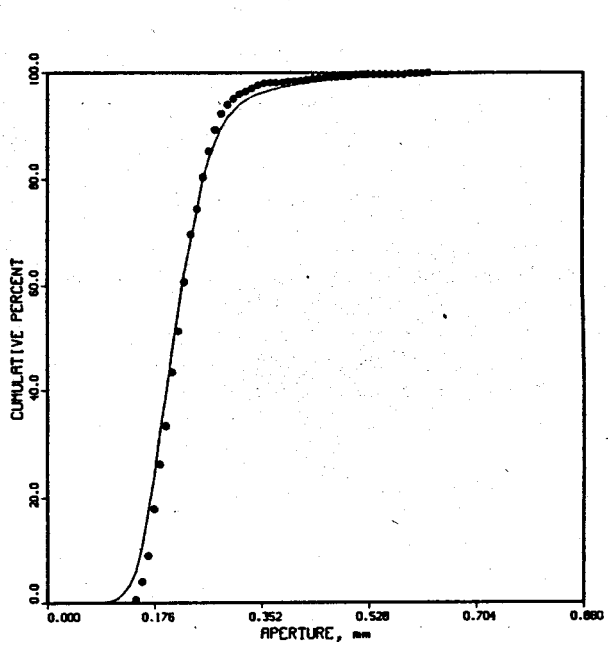

Figure 1. Cumulative aperture distribution for fracture from Dixie Valley, Nevada, for 1024×1024 data set (solid line) and 32×32 reduced data set (dots).

DISCUSSION OF THE APERTURE DISTRIBUTION

One feature that is obvious from the contour plot (Fig.2) is the anisotropy in the data, both along the sliding direction (the x-direction), and along the direction orthogonal to the sliding direction (the y-direction). There is generally a longer-range spatial correlation in the x-direction. Small discrete linear features are present, that are elongated along the sliding direction. These correspond to lithic clasts seen on the footwall side of the fracture surface, and the greatest apertures occur as isolated peaks near these discontinuities. A larger-scale mild anisotropy in the y-direction is apparent in the trend from thickest apertures at the top to thinnest apertures at the bottom. This has very important effects on multi-phase flow (see below).

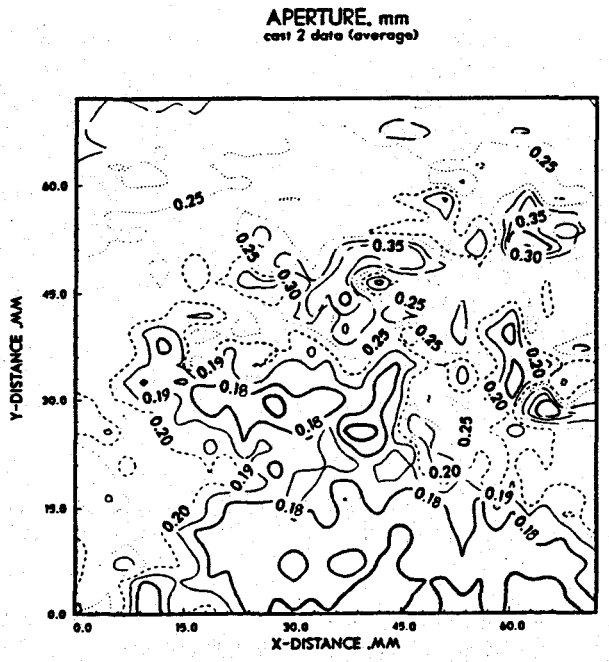

Figure 2. Contour diagram of fracture apertures, as determined from digital image analysis.

The description of fracture void geometry obtained by the casting method should be considered preliminary at present. The process from excavating the fracture specimen in the field to eventually arriving at a pixel-by-pixel definition of apertures from the cast involves many potential sources of inaccuracies and systematic errors, which have not yet been quantified. Possible sources of error include imperfect mating of fracture walls in the casting procedure, imperfections in the cast itself (air bubbles, tearing, dust particles), non-uniform lighting conditions when digitizing, and inaccuracies in the calibration of cast thickness versus light attenuation.

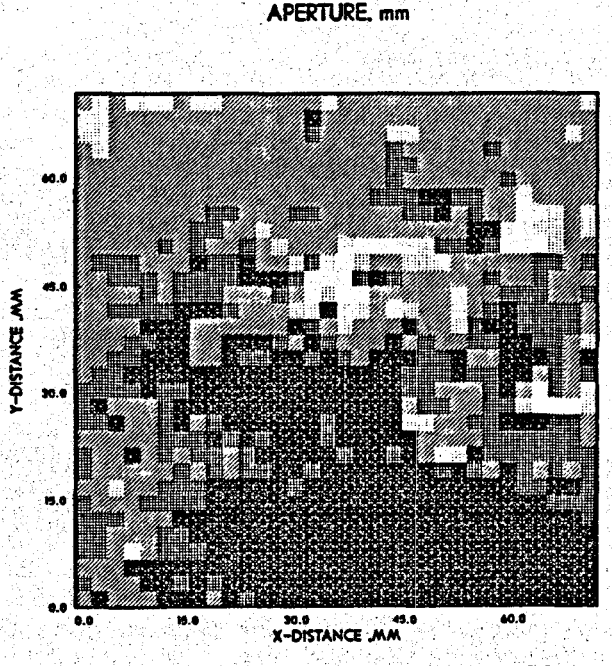

Figure 3. A 32 × 32 discretized representation of fracture apertures. Lighter shading corresponds to larger apertures.

RELATIVE PERMEABILITY ANALYSIS

From the geometric description of the fracture void space, a theoretical prediction of two-phase relative permeabilities has been developed, using the approach of Pruess and Tsang (1989a, 1989b). This approach can be briefly summarized as follows. The starting point is a discretized description of fracture apertures, as has been obtained here through digital image analysis on fracture casts (Fig. 3). A "local parallel-plate approximation" is then made to determine phase occupancy of different fracture segments, and to calculate their permeability. Specifically, at some given capillary suction pressure P_c, all fracture segments with apertures $b > b_c = 2\gamma/P_c$ are assumed to be occupied by non-wetting phase, all apertures $b < b_c$ are occupied by wetting phase. The corresponding wetting phase saturation $S_w(b_c)$ is calculated by directly summing over the volumes of all fracture segments with $b < b_c$, and dividing by the total fracture void volume. Strictly speaking, in addition to capillary "allowability," which is a purely local criterion, phase occupancy will also be affected by global "accessibility." Indeed, phase occupancy of a fracture segment can change only if the "other" phase can access the segment through a contiguous pathway from the system boundaries. Accessibility will give rise to hysteresis (path dependence) of phase occupancy and permeability; these effects have been neglected here to simplify the analysis.

After the phase occupancy for given capillary suction conditions has been decided, effective permeabilities to wetting and non-wetting phases are calculated by applying a suitable pressure drop across the fracture, and simulating steady single-phase flow in the network of occupied fracture segments. Two separate single-phase flow simulations are performed to obtain, respectively, the steady-state flow rate $F_w(b_c)$ when only apertures less than b_c are occupied, and the steady-state flow rate $F_{nw}(b_c)$ when only apertures larger than b_c are occupied. Denoting the flow rate when all fracture segments are occupied with F_o, the wetting and non-wetting phase relative permeabilities at aperture cutoff b_c, corresponding to wetting phase saturation $S_w(b_c)$, are given by, respectively,

$$k_w(S_w) = F_w(S_w)/F_o \qquad (1a)$$

$$k_{nw}(S_w) = F_{nw}(S_w)/F_o \ . \qquad (1b)$$

The approximation of treating the two-phase flow problem in the fracture plane as two separate single-phase flow problems will be valid only under conditions of small capillary number (capillary forces dominating over viscous drag). Other limitations and approximations in this approach to fracture relative permeabilities are discussed in Pruess and Tsang (1989a, 1989b).

RESULTS FOR FRACTURE RELATIVE PERMEABILITIES

In the first set of simulations we evaluated relative permeabilities for flow in the x-direction (see Fig. 3), with no-flow boundaries maintained at the upper and lower edge of the fracture. Results given in Fig. 4 indicate that both wetting and non-wetting phase relative permeability curves are not much different from customary porous medium relative permeabilities. This is especially true for the wetting phase relative permeability, which has a familiar shape and an irreducible saturation $S_{wir} = 30\%$. The non-wetting curve is approximately linear, with an irreducible saturation of $S_{nwir} = 36\%$. This value is larger than commonly encountered in porous media, but smaller than the values previously obtained for artificial computer-generated fractures. Note that there is a broad saturation "window" in which both phases can flow simultaneously. This occurs because of the long-range spatial correlations between fracture apertures in the x-direction (see Fig. 3), and the partial segregation of large (near the top) and small (near the bottom) apertures.

Simulated relative permeabilities in both the x- and y-directions are plotted in Fig. 5. These relative permeabilities are generally much smaller, and there is a broad saturation gap in which neither phase can flow. Note that the saturation at which wetting phase flow ceases in the x-direction coincides with the onset of non-wetting phase flow in the transverse (y-) direction. Wetting phase percolation in y-direction is not possible until after wetting saturation rises beyond the point at which non-wetting phase flow terminates in the x-direction. Within the approximations of our local capillary equilibrium model, it is clear that as long as a fluid

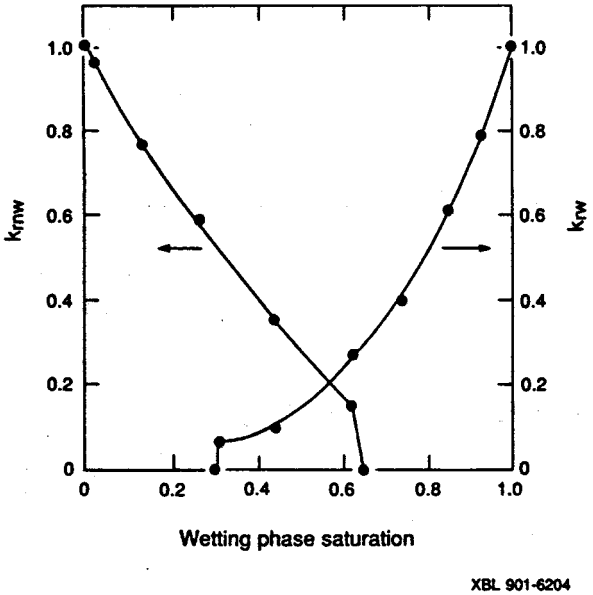

Figure 4. Simulated relative permeabilities for flow in the x-direction (see Fig. 3).

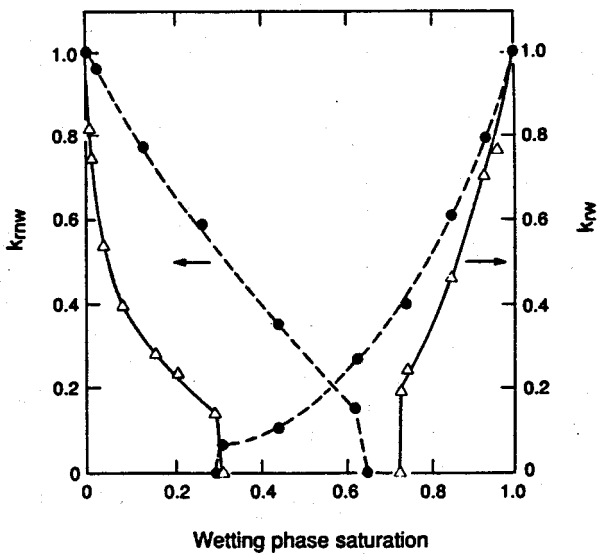

Figure 5. Simulated relative permeabilities for flow in the x-direction (dashed line) and y-direction (solid line) (see Fig. 3).

phase can flow in a certain direction, the other phase can not flow in the perpendicular direction. This "percolation exclusion" is a direct consequence of the two-dimensional nature of the pore space.

In the third set of relative permeability simulations we applied a shift

$$b \rightarrow b' = b - \Delta b$$

to all apertures, to simulate conditions of fracture closure. This case can also shed light on the sensitivity of fracture relative permeability predictions to unavoidable systematic errors in the cast thickness versus light attenuation calibration. A shift of $\Delta b = 0.15$ mm is applied, reducing seven out of the total of 1024 apertures to zero. Results for the relative permeabilities of the shifted fracture for flow in x-direction are given in Fig. 6. It is remarkable that for much of the saturation range there is very little change in either wetting or non-wetting phase relative permeability. The main differences occur near the irreducible saturations. On approach to the irreducible wetting phase saturation wetting phase relative permeability is diminished, but the irreducible saturation itself has declined to a very small 15 percent, compared with 30 percent for the unshifted fracture. Irreducible non-wetting phase saturation has increased from $S_{nwir} = 36\%$ to $S_{nwir} = 53\%$. A simple algebraic derivation shows that, when all apertures are decreased by the same amount, the wetting phase saturation at both the wetting and non-wetting phase percolation thresholds will always be reduced. This is an important result, indicating that in small microcracks contiguous flow paths for wetting phase may exist even at small values of liquid saturation (large capillary suction pressures).

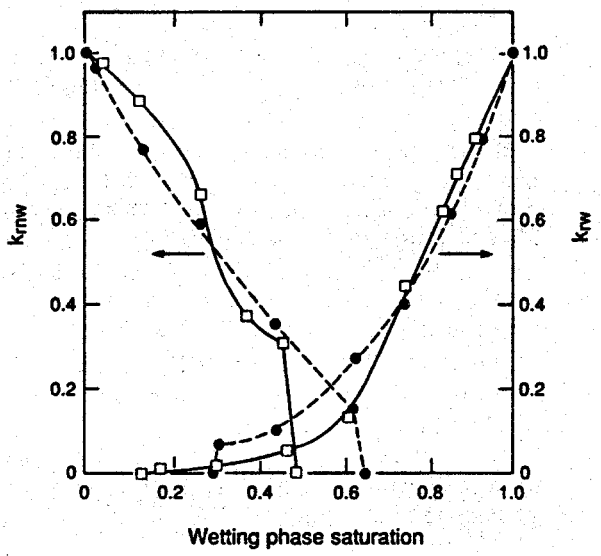

Figure 6. Simulated relative permeabilities in the x-direction, with all apertures reduced by 0.150 mm (solid line). Dashed line is for flow in x-direction without aperture reduction.

DISCUSSION AND CONCLUSIONS

Several recent studies of natural fractures in hard rock have documented the crucial role of wall roughness, and the consequent irregular nature of the void space enclosed between the fracture walls (Brown and Scholz, 1985; Gentier, 1986; Pyrak-Nolte *et al.*, 1987, 1988; Gale, 1987; Hakami, 1988). The conventional picture of fractures as parallel plates has been replaced by an appreciation of the strong analogy, as well as important differences, between the void space geometries of fractures and (three-dimensional) porous media. Recent studies of single and multiphase flow and transport behavior of rough-walled rock fractures have employed the conceptualization of two-dimensional heterogeneous porous media (Tsang and Tsang, 1987; Brown, 1987; Tsang and Tsang, 1989; Pruess and Tsang, 1989a,b). Predictions derived from these approaches can be no more realistic than the description of fracture void space geometry on which they are based, thus placing a premium on acquiring good data for fracture aperture distributions.

In the present work we have employed a casting technique to replicate and quantify the void space geometry of a rock fracture from Dixie Valley, Nevada. We have then utilized the geometry data to develop, for the first time, a prediction of the relative permeability behavior of an actual rock fracture. Our predictions are approximate and preliminary; among other things they ignore phase transformation effects (boiling and condensation). Such effects are expected to significantly enhance vapor relative permeability in geothermal reservoirs in comparison to non-wetting phase relative permeability in two-component flow systems, such as water-oil or water-noncondensible gas (Verma, 1986).

The void space geometry of the fracture analyzed here differs greatly from previous computer-generated fractures for which flow and transport predictions were made (Pruess and Tsang, 1989a, b). Computer-generated aperture distributions have usually been specified as lognormal, leading to a highly asymmetric distribution with a preponderance of small apertures. In contrast, our fracture is completely open, with a smallest aperture of 0.141 mm; the distribution is fairly narrowly peaked around 0.200 mm. In spite of this strong difference, the predicted wetting phase relative permeability is similar to previous results for computer-generated fractures and to generally accepted relative permeabilities for porous media (Pruess and Tsang, 1989a, b). Non-wetting phase relative permeability was found to depend on non-wetting phase saturation in similar fashion as wetting phase relative permeability depends on wetting phase saturation. A strong anisotropy in relative permeability behavior was noted, which is explained by the highly anisotropic spatial correlations between apertures. Calculations for an assumed closure of the fracture (decreasing all apertures by the same amount, equal to the smallest aperture) gave surprising results. For large values of saturation, relative permeabilities for either wetting or non-wetting phase changed very little. The irreducible saturation decreased for the wetting and increased for the non-wetting phase. This suggests that in small fractures with numerous asperity contacts contiguous liquid flow paths will exist even at small values of liquid saturation (strong capillary suction conditions).

Our studies are continuing. An essential task not yet accomplished is the direct experimental demonstration that multiphase flow in a rough-walled rock fracture can in fact be adequately predicted on the basis of void space geometry averaged over areas of several mm^2. Construction of a laboratory flow apparatus for this purpose is underway. Important issues also remain to be addressed in fracture geometry measurement, and in a more complete and rigorous modeling of multiphase flow within a known void space geometry.

ACKNOWLEDGEMENT

The authors appreciate helpful discussions with Bill Power, Yvonne Tsang, Joe Wang, and Larry Myer. For a careful review of the manuscript, we are indebted to Yvonne Tsang and Larry Myer. This work was supported by the Geothermal Technology Division, and by the Office of Civilian Radioactive Waste Management, U.S. Department of Energy, under Contract No. DE-AC03-76SF00098. Support for the numerical computations was provided by the Office of Basic Energy Sciences, U.S. Department of Energy.

REFERENCES

Cox, B. L., Persoff, P., Power, W. L. *et al.*, 1990. "Single Fracture Geometry by Optical and Mechanical Methods: A Comparison," in progress.

Brown, S. R., 1987. "Fluid Flow Through Rock Joints: The Effect of Surface Roughness," *J. Geophys. Res., 92*, (B2), 1337–1347.

Brown, S. R. and C. H. Scholz, 1985. Broad bandwidth study of the topography of natural rock surfaces, *J. Geophys. Res., 90*, 12, 575–12,582.

Gale, J. E., 1987. Comparison of coupled fracture deformation and fluid flow models with direct measurements of fracture pore structure and stress-flow properties, *Proceedings, 28th U.S. Symposium on Rock Mechanics*, Tucson, AZ, June 29–July 1, pp. 1213–1222.

Gentier, S., 1986. Morphologie et comportement hydromécanique d'une fracture naturelle dans un granite sous contrainte normale, Doctoral thesis, Université d'Orléans, Orléans, France.

Gentier, S., D. Billaux, and L. van Vliet, 1989. Laboratory testing of the voids of a fracture, Rock Mechanics and Rock Engineering, 22, 149-157.

Hakami, E., 1988. Water flow in single rock joints, *Licentiate Thesis*, Lulea University of Technology, Lulea, Sweden, November.

Power, W. L. and T. E. Tullis, 1989. The relationship between slickenside surfaces in fine-grained quartz and the seismic cycle, submitted to *J. Struc. Geol.*.

Pruess, K. and Y. W. Tsang, 1989a. On relative permeability of rough-walled fractures, *Transactions of the Fourteenth Annual Workshop on Geothermal Reservoir Engineering*, Stanford, CA, January 24–26, 1989.

Pruess, K. and Y. W. Tsang, 1989b. On Two-phase relative permeability and capillary pressure of rough-walled rock fractures, Lawrence Berkeley Laboratory report LBL-27449, submitted to Water Resources Research.

Pyrak-Nolte, L. J., L. R. Myer, N. G. W. Cook, and P. A. Witherspoon, 1987. Hydraulic and mechanical properties of natural fractures in low permeability rock, *paper presented at Sixth International Congress on Rock Mechanics*, Montreal, Canada, August.

Pyrak-Nolte, L. J., Cook, N. G. W., and D. D. Nolte, 1988. Fluid percolation through single fractures, *Geophys. Res. Lett., 15*, 1247–1250.

Tsang, Y. W. and C. F. Tsang, 1987. Channel model of flow through fractured media, *Water Resources Res., 23*, (3), 467–479.

Tsang, Y. W. and C. F. Tsang, 1989. Flow channeling in a single fracture as a two-dimensional strongly heterogeneous permeable medium, *Water Resources Res., 25*, (9), 2076–2080.

Verma, A. K., 1986. Effects of Phase Transformation on Steam-water Relative Permeabilities, PhD dissertation, University of California, Berkeley, CA., LBL-20594.